

Evidence for Coexistence of the Superconducting Gap and the Pseudogap in Bi-2212 from Intrinsic Tunneling Spectroscopy

V.M. Krasnov,^{1,2} A. Yurgens,^{1,3} D. Winkler,^{1,4} P. Delsing,¹ and T. Claeson¹

¹*Department of Microelectronics and Nanoscience, Chalmers University of Technology, S-41296 Göteborg, Sweden*

²*Institute of Solid State Physics, 142432 Chernogolovka, Russia*

³*P.L. Kapitza Institute, 117334 Moscow, Russia*

⁴*IMEGO Institute, Aschebergsgatan 46, S41133 Göteborg, Sweden*

(Received 11 February 2000)

We present intrinsic tunneling spectroscopy measurements on small $\text{Bi}_2\text{Sr}_2\text{CaCu}_2\text{O}_{8+x}$ mesas. The tunnel conductance curves show both sharp peaks at the superconducting gap voltage and broad humps representing the c -axis pseudogap. The superconducting gap vanishes at T_c , while the pseudogap exists both above and below T_c . Our observation implies that the superconducting and pseudogaps represent different coexisting phenomena.

PACS numbers: 74.25.Jb, 74.50.+r, 74.72.Hs, 74.80.Dm

The existence of a pseudogap (PG) in the quasiparticle density of states (DOS) in the normal state of high- T_c superconductors (HTSC) has been revealed by different experimental techniques [1–9]. For a review, see Refs. [9–12]. There is presently no consensus about the origin of the PG, the correlation between the superconducting gap (SG) and PG, or the dependencies of both gaps on material and experimental parameters. A clarification of these issues is certainly important for understanding HTSC.

From surface tunneling experiments, it was concluded that the SG is almost temperature independent [1,5]. At $T > T_c$, it continuously evolves into the PG, which can persist up to room temperature. Furthermore, it was observed that such a superconducting gap has no correlation with T_c and continues to increase in underdoped samples despite a reduction of T_c [1,2,5]. This was the basis for a suggestion that the PG state at $T > T_c$ is a precursor of superconductivity [10]. On the other hand, surface tunneling into HTSC has several drawbacks [13]; e.g., it is sensitive to surface deterioration. The growing controversy requires studies with alternative techniques.

Intrinsic tunneling spectroscopy has become a powerful tool in studying the quasiparticle DOS *inside* bulk single crystals of layered HTSC [4,8,14–17] and is thus unsusceptible to surface deterioration. First experiments have been recently attempted [4,15,16] to study the PG in mesas fabricated on the surface of $\text{Bi}_2\text{Sr}_2\text{CaCu}_2\text{O}_{8+x}$ (Bi-2212) single crystals. Unfortunately, intrinsic tunneling experiments also have several problems, such as internal heating and stacking faults (defects) in the mesas. To reduce overheating, a pulse technique was applied by Suzuki *et al.* [4]. The result at $T \sim T_c$ was essentially similar to the surface measurements [1], leaving the obscure relationship between SG and PG [4,15] unresolved.

In this paper we present results of intrinsic tunneling spectroscopy for Bi-2212 mesas with considerably smaller areas, compared to previous studies [4,15]. Smaller areas allowed us to avoid stacking faults in the mesas and

to avoid mixing between the c -axis and ab -plane transport. As a result, clean and clear tunnel-type current-voltage (I - V) characteristics were observed, which allowed us to distinguish superconducting and pseudogaps in a wide range of temperatures. In contrast to surface and earlier intrinsic tunneling experiments [1,4,15], we have clearly traced different behaviors of the SG and PG. Thorough studies of I - V curves close to T_c revealed that the superconducting gap does vanish, while the PG does not change at $T = T_c$. All this speaks in favor of different origins of the two coexisting phenomena and against the precursor-superconductivity scenario of the PG. Finally, we discuss interplay between Coulomb interaction and low dimensionality as a possible mechanism for the c -axis PG in an inherent two-dimensional (2D) system, such as the Bi-2212 single crystals.

Mesas with different dimensions from 2 to 20 μm were fabricated simultaneously on top of Bi-2212 single crystals. To reduce the mesa area we adopted a self-alignment technique (see Ref. [17] for details of sample fabrication). The c -axis I - V characteristics were measured in a three-probe configuration. The contact resistance was small, about 2 orders of magnitude less than the total resistance of the mesa at the corresponding current. Altogether, more than 50 mesas made on different crystals were investigated. Parameters of the mesas are listed in Table I. Here we present results for slightly overdoped ($T_c = 89$ K) and optimally doped ($T_c = 93$ – 94 K) samples. The pristine crystals were slightly overdoped. Overdoped mesas were obtained by wet chemical etching. Optimally doped mesas were made by Ar-ion etching, during which mesas partly loose oxygen. Such mesas had larger T_c , c -axis resistivity ρ_c (see Table I), and PG [see Fig. 4 (below)].

Our fabrication procedure is highly reproducible. This is illustrated in the top inset of Fig. 1, in which current density, $j = I/S$, vs voltage per junction, $v = V/N$, curves at $T = 4.2$ K are shown for three mesas with different areas from different batches and crystals. Here S is the

TABLE I. Parameters of Bi-2212 mesas, ρ_c is the c -axis normal-state resistivity at large bias. The three figures in the mesa number represent the batch number, the crystal number, and the number of the mesa on the crystal, respectively. Letters "Ar" or "Ch" indicate whether the mesa was made by Ar-ion or wet chemical etching.

Mesa	S (μm^2)	N	T_c (K)	$\Delta_s(0)$ (meV)	$\delta v_s(0)$ (mV)	$\rho_c(4.2\text{ K})$ ($\Omega\text{ cm}$)
423Ar	3.5×7.5	10	93	33.3	38.5	44.9
255Ar	5.5×6	12	92.5	32.5	35.5	45.4
251Ar	6×6	12	92.5	32.5	35.5	44.5
211Ar	4×7.5	12	94	33.0	37	44.0
216Ar	4×20	10	94	32.3	38.5	44.9
015Ch	12×15	9	89	25.8	28.5	32.3

area and N is the number of intrinsic Josephson junctions (IJJ's) in the mesa. We note that all normalized I - V curves collapse into a single curve. In the following, we will denote quantities corresponding to the whole mesa by capital letters, and those related to an individual IJJ by small letters. The subscripts "s," "pg," and "n" will correspond to the superconducting, pseudogap, and normal state properties, respectively.

In Fig. 1, I - v curves and, in Fig. 2, the voltage dependence of the dynamic conductance $\sigma(v) = dI/dv(v)$ are shown for the optimally doped mesa 423Ar at different temperatures. Figures 1 and 2 exhibit a typical tunnel-junction behavior. At large bias current, there is a well-defined normal-state part of tunneling I - V curves with tunnel resistance R_n . R_n , obtained at the largest bias, $v \approx 150$ mV, decreases by merely $\sim 15\%$ from 300 to 4.2 K and has no feature at $T = T_c$, as shown in the

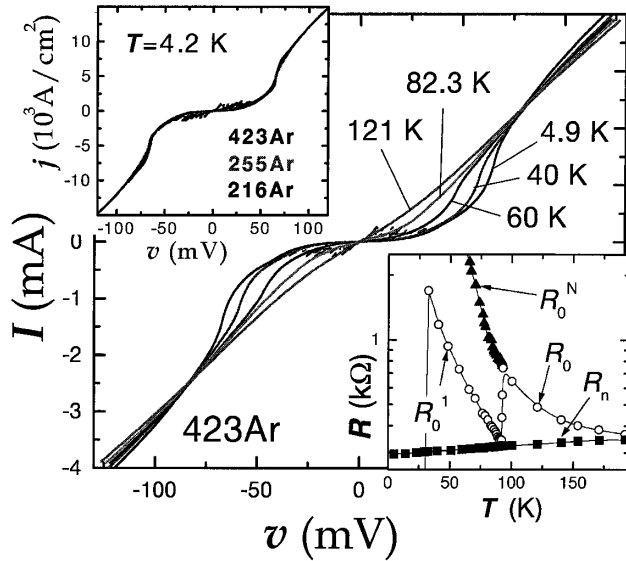


FIG. 1. I - v curves for the 423Ar mesa at different T . Top inset shows normalized I - V curves at $T = 4.2$ K for three different mesas. Bottom inset shows in the logarithmic scale temperature dependencies of the zero bias resistance R_0 (open circles), large bias resistance R_n (solid squares) and the total subgap resistance R_0^N (solid triangles).

bottom inset of Fig. 1. This is in accordance with the pure tunnel-junction behavior, for which R_n is expected to be temperature independent. The weak T dependence of R_n indicates an absence of mixing between c -axis and ab -plane transport in our mesas. Previously, however, a strong change of R_n at $T = T_c$ has been reported for larger mesas [4,15]. On the other hand, the zero bias resistance R_0 has a strong temperature dependence (see bottom inset in Fig. 1). Below T_c , R_0 is determined by the subgap resistance of the first IJJ, R_0^1 . At $T < 40$ K, a small critical current in the first IJJ appears [see Fig. 3(a)], and R_0 drops to the contact resistance. Such a two stage decrease of R_0 is due to a deterioration of IJJ's at the surface of the mesa [18].

At low T , there is a sharp peak in $\sigma(v)$, which we attribute to the superconducting gap voltage [19], $v_s = 2\Delta_s/e$. With increasing T , the peak at v_s reduces in amplitude and shifts to lower voltages, reflecting the decrease in $\Delta_s(T)$. At $T \sim 83$ K ($< T_c \approx 93$ K), the superconducting peak is smeared out completely and only a smooth depletion of $\sigma(0)$ (a dip) plus a hump in conductance at $v = v_{pg} \approx 70$ mV remain. The dip and the hump are correlated to each other and both flatten simultaneously with increasing T (see inset in Fig. 2). Therefore, both reflect the existence of the pseudogap in the tunneling DOS. The $\sigma(0)$ gradually increases with temperature but the I - V curves remain nonlinear nearly up to room temperature. At $T > T_c$, the zero-bias resistance, R_0 , can be fairly well described by the thermal-activation formula, $R_0 \propto \exp(T^*/T)$, $T^* \approx 150 \pm 20$ K.

In agreement with surface tunneling experiments [1,2], there are no sharp changes at T_c . As shown in the bottom inset of Fig. 1, at $T < T_c$, R_0 evolves continuously into the total (all N junctions in the resistive state) subgap

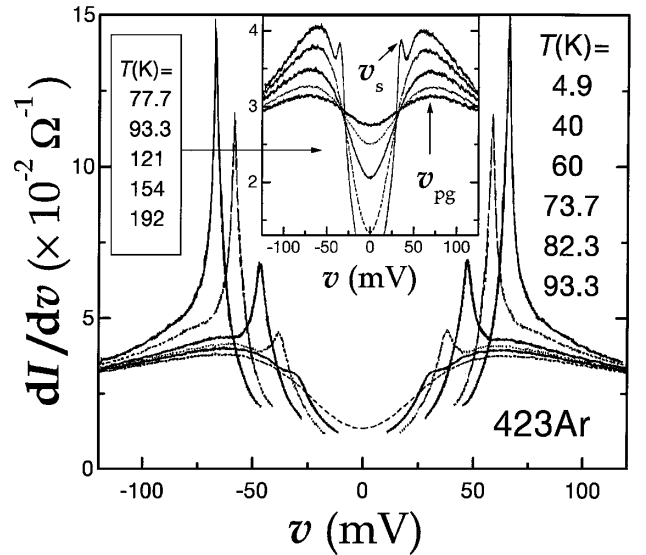


FIG. 2. Dynamic conductance, $\sigma(v)$, at different temperatures for 423Ar mesa. Inset shows detailed curves for high T . Coexistence of the superconducting peak, v_s , and the pseudogap hump, v_{pg} , is clearly visible at $T = 77.7$ K.

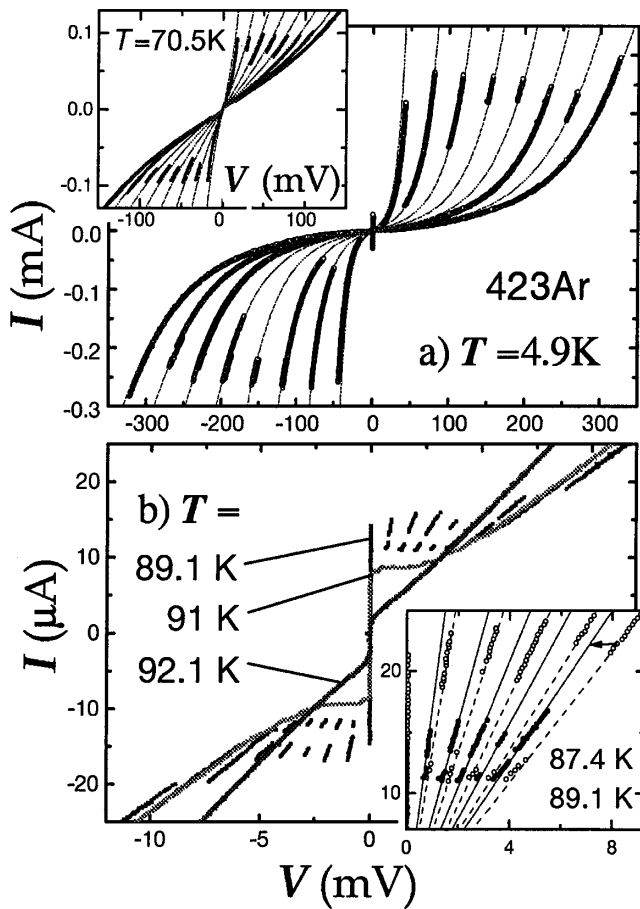


FIG. 3. Detailed views of quasiparticle branches for the 423Ar mesa at different temperatures. Thin lines in (a) represent polynomial fits and indicate good scaling of QP branches. The inset in (b) shows the first five QP branches at T close to T_c , in an expanded scale. The arrow demonstrates the tendency for vanishing $\delta v_s(T)$ at $T \rightarrow T_c$ even when measured at one and the same current.

resistance, R_0^N . This implies that the PG persists also in the superconducting state. The gradual evolution of the PG hump upon cooling through T_c is most clearly shown in the inset of Fig. 2. It is seen that the PG dip/hump feature does not change qualitatively upon cooling through T_c . Moreover, the I - V curve at $T = 77.7$ K shows that the superconducting peak at v_s emerges on top of the PG—features which demonstrates a coexistence of both SG and PG features. From Fig. 2 it is seen that, with decreasing temperature, the superconducting peak shifts to higher voltages, increases in amplitude, and eventually the PG hump is washed out by the much stronger superconducting peak. For optimally doped mesas, the PG hump can be resolved at $T > 60$ K, i.e., well below T_c . The gradual opening of Δ_s at $T < T_c$, in addition to the PG, can also be seen from a steeper growth of the total subgap resistance R_0^N at $T < T_c$, as compared to the thermal-activation behavior of R_0 at $T \geq T_c$.

At low bias and $T < T_c$, multiple quasiparticle (QP) branches are seen in the I - V curves, representing a one-by-one switching of the IJJ's into the resistive state [4,14]. A

detailed view of multiple QP branches is shown in Fig. 3 for different T . Dots and thin lines in Fig. 3(a) represent the experimental points and a polynomial fit, correspondingly. Only the last branch, having many data points, was actually fitted; all the other thin lines were obtained by dividing the voltages of this fit, $V_{\text{fit}}(I)$, by the integer number $N^* = N - n + 1$, where n is the number of IJJ's in the resistive state. A good scaling of QP branches is seen, which implies that there is no significant overheating of the mesa at the operational current. If there were overheating, $V_{\text{fit}}(I)/N^*$ would not go through the data points because switching of additional IJJ's would cause a progressive increase of the internal temperature and the branches with increasing count numbers would have lower voltages due to the strong temperature dependence of R_0^N and Δ_s .

The separation between QP branches, δv_s , is the additional quantity, provided by intrinsic tunneling spectroscopy, which can be used to estimate Δ_s in a wider range of temperatures. From Fig. 3(b) it is seen that multiple QP branches are clearly distinguishable up to $T \sim T_c - 2$ K. From Table I it is seen that δv_s scales with Δ_s . The δv_s is less than V_s/N simply because the critical current, I_c , is less than V_s/R_n and all IJJ's switch to the resistive state before they reach the gap voltage (see Fig. 1). The $\delta v_s(I = I_c)$ continuously decreases with T and vanishes at T_c . In principle, the temperature dependence of I_c is also involved in $\delta v_s(T)$, since we measure δv_s at $I \approx I_c$. However, the inset in Fig. 3(b) reveals that $\delta v_s(T)$ still tends to vanish at $T \rightarrow T_c$ even if we evaluate δv_s at one and the same current for all T .

In Fig. 4, the temperature dependencies of the superconducting peaks, v_s (squares), $\delta v_s(I = I_c)$ (circles), and pseudogap humps, v_{pg} (triangles), are shown for optimally doped (solid) and overdoped (open symbols) samples. Small solid symbols represent v_s for the rest of the mesas listed in Table I, and the lines are guides for the eye. In agreement with previous studies, both v_s and v_{pg} increase upon going from overdoped to optimally doped samples [1,2,5]. The superconducting gap deduced from the sum-gap voltage $V_s = 2N\Delta_s/e$ is $\Delta_s(4.2 \text{ K}) \approx 33$ meV for the optimally doped sample, and ≈ 26 meV for the overdoped one. In contrast to surface tunneling experiments, we observe that Δ_s decreases considerably with temperature. The robust decrease of $\Delta_s(T)$ from 4.2 K to T_c is more than 80% for the overdoped mesas. Moreover, we can measure $\delta v_s(I = I_c)$ in a wider range of T and observe that it vanishes at $T \rightarrow T_c$.

All this brings us to the conclusion that the superconducting gap does close at T_c , in agreement with the previous observations of vanishing of the superfluid density (divergence of the magnetic penetration depth) [20] and the Josephson plasma frequency [21]. On the contrary, the PG is almost temperature independent and exists both above and below T_c . Therefore, the SG is not developing from the PG, and these two gaps represent different coexisting phenomena. The recently observed independence of the PG on magnetic field [7] supports our conclusion and also

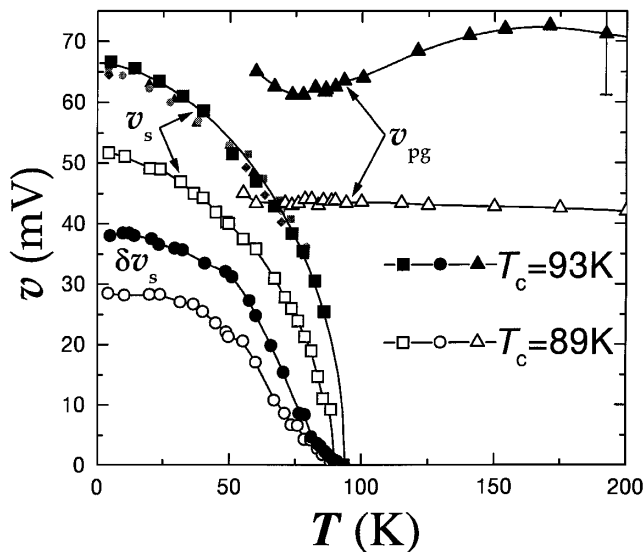


FIG. 4. Temperature dependence of parameters of the optimally doped (solid symbols) and overdoped (open symbols) samples: the superconducting peak voltage, $v_s = 2\Delta_s/e$, the spacing between QP branches, δv_s , and the pseudogap hump voltage, v_{pg} . It is seen that the superconducting gap vanishes at T_c , while the pseudogap exists both above and below T_c .

casts doubts about the precursor-superconductivity origin of the PG [10].

One possible “nonsuperconducting” PG scenario is the formation of charge or spin density waves (CDW or SDW) [6,11]. HTSC’s are composed of quasi-two-dimensional electronic systems with a certain degree of Fermi-surface nesting [6], which can make the system unstable with respect to CDW or SDW formation [22,23]. A CDW or SDW is accompanied by a PG in DOS, detectable by a surface-tunneling spectroscopy [24]. Many similarities exist between the PG in CDW or SDW (including ARPES [23], optical conductivity, and NMR [11,22]) and the PG in HTSC. On the other hand, an opening of the PG due to CDW or SDW is typically accompanied by an increase in the resistivity [22], while the opposite tendency was observed in HTSC [25].

We would also like to emphasize a similarity between the PG features of c -axis tunneling in HTSC and Coulomb PG for tunneling into a two-dimensional electron system (2DES). The Coulomb PG in 2DES is well studied in connection with semiconducting heterostructures [26–28]. Experimental $\sigma(v)$ curves from the inset in Fig. 2 are strikingly similar to “V-shaped” tunneling characteristics of 2DES [26,27]. Certainly, the electron system in Bi-2212 is highly two dimensional. Moreover, a Coulomb origin of the HTSC pseudogap would naturally explain the increase of PG with decreasing O-doping and carrier concentration. A large Coulomb PG in low conducting 2DES is due to unscreened long-range Coulomb interaction [27] and/or slow charge accommodation [28]. Large PG could also appear if tunneling occurs via intermediate low conducting BiO layers [12].

An attractive feature of both CDW/SDW and Coulomb PG scenarios is that the PG can persist in the superconducting state [24]. Below T_c , SG and PG are combined into a larger overall gap [11]. This is in agreement with a definite trend for the increase of v_{pg} at $T < T_c$ (see Fig. 4). This might also help in the understanding of large “superconducting” gaps seen in underdoped HTSC [1,2]. Whether the CDW/SDW or Coulomb PG scenarios can explain all PG features in HTSC remains to be clarified.

In conclusion, small mesa structures were used for intrinsic tunneling spectroscopy of Bi-2212. We were able to distinguish and simultaneously observe both superconducting and pseudogaps in a wide range of temperatures. The superconducting gap has a strong temperature dependence and vanishes at T_c , while the pseudogap is almost temperature independent and exists both above and below T_c . This suggests that the pseudogap is not directly related to superconductivity.

- [1] Ch. Renner *et al.*, Phys. Rev. Lett. **80**, 149 (1998).
- [2] N. Miyakawa *et al.*, Phys. Rev. Lett. **83**, 1018 (1999).
- [3] J. W. Loram *et al.*, Phys. Rev. Lett. **71**, 1740 (1993).
- [4] M. Suzuki *et al.*, Phys. Rev. Lett. **82**, 5361 (1999).
- [5] M. R. Norman *et al.*, Phys. Rev. B **57**, R11093 (1998).
- [6] N. L. Saini *et al.*, Phys. Rev. Lett. **79**, 3467 (1997).
- [7] K. Gorny *et al.*, Phys. Rev. Lett. **82**, 177 (1999).
- [8] A. Yurgens *et al.*, cond-mat/9907159.
- [9] A. V. Puchkov *et al.*, J. Phys. Condens. Matter **8**, 10049 (1996).
- [10] M. Randeira, cond-mat/9710223.
- [11] R. S. Markiewicz *et al.*, Phys. Rev. B **60**, 627 (1999).
- [12] J. Halbritter, Physica (Amsterdam) **302C**, 221 (1998).
- [13] P. Mallet *et al.*, Phys. Rev. B **54**, 13324 (1996).
- [14] K. Schlenga *et al.*, Phys. Rev. B **57**, 14518 (1998).
- [15] I. F. G. Parker *et al.*, Proc. SPIE Int. Soc. Opt. Eng. **3480**, 11 (1998).
- [16] D. Winkler *et al.*, Supercond. Sci. Technol. **12**, 1013 (1999).
- [17] V. M. Krasnov *et al.*, cond-mat/0002094.
- [18] N. Kim *et al.*, Phys. Rev. B **59**, 14639 (1999).
- [19] We measure angular average characteristics. In the case of the d -wave superconductor, the peak would represent the maximal gap at $\phi = 0$ (see, e.g., Ref. [11]).
- [20] S. F. Lee *et al.*, Phys. Rev. Lett. **77**, 735 (1996).
- [21] T. Shibauchi *et al.*, Phys. Rev. Lett. **83**, 1010 (1999).
- [22] G. Grüner, *Density Waves in Solids* (Addison-Wesley, Reading, MA, 1994).
- [23] G. H. Gweon *et al.*, J. Phys. Condens. Matter **8**, 9923 (1996).
- [24] H. F. Hess *et al.*, Phys. Rev. Lett. **64**, 2711 (1990); Z. Dai *et al.*, Phys. Rev. B **48**, 14543 (1993).
- [25] T. Watanabe *et al.*, Phys. Rev. Lett. **79**, 2113 (1997).
- [26] H. B. Chan *et al.*, Phys. Rev. Lett. **79**, 2867 (1997); V. T. Dolgoplov *et al.*, *ibid.* **79**, 729 (1997).
- [27] F. G. Pikus and A. L. Efros, Phys. Rev. B **51**, 16871 (1995).
- [28] L. S. Levitov and A. V. Shitov, JETP Lett. **66**, 215 (1997).